Quantized Majorana pump in semiconductor-superconductor heterostructures

Hui Tan,[1] Pei-Hao Fu,[2] Yan-Ru Chen,[2] Jun-Feng Liu,[1,*] Jun Wang,[3,†] and Zhongshui Ma[4,5]

[1]*School of Physics and Materials Science, Guangzhou University, Guangzhou 510006, China*
[2]*Department of Physics, Southern University of Science and Technology, Shenzhen 518055, China*
[3]*Department of Physics, Southeast University, Nanjing 210096, China*
[4]*School of Physics, Peking University, Beijing 100871, China*
[5]*Collaborative Innovation Center of Quantum Matter, Beijing 100871, China*

(Received 12 January 2021; revised 19 April 2021; accepted 19 April 2021; published 6 May 2021)

We propose a quantized Majorana pump (QMP) in semiconductor-superconductor heterostructures. The pump consists of a Majorana nanowire, i.e., a Rashba wire in proximity to an *s*-wave superconductor and in a magnetic field, and two ferromagnetic leads. When the orientation of the magnetic field is rotated by 2π, an elementary charge e is transferred between two leads. The number of the pumped charge in a cycle is related to the winding number of the Andreev reflection amplitude. In the topologically trivial phase without Majorana zero mode (MZM), the pumped charge decreases rapidly to zero. More importantly, the pump works at zero bias and provides a more effective way to distinguish MZMs from trivial partially separated Andreev bound states. Therefore, this QMP provides not only a smoking-gun signature of MZMs, but also an ideal platform to realize topological single-electron pumps with the potential for realizing novel current standards in electrical metrology.

DOI: 10.1103/PhysRevB.103.195407

I. INTRODUCTION

The emergence of Majonana zero modes (MZMs) at the boundary of topological superconductors has been attracting a lot of interest for potential applications in topological quantum computations due to their non-Abelian exchange property [1–10] . But the conclusive evidence of MZMs has not yet been observed in experiments. The experimental observation of quantized Majorana conductance (QMC) in semiconductor-superconductor heterostructures has proved to be a hard task [11,12]. And theoretically, the QMC has been shown to may arise owing to trivial partially separated Andreev bound states (PSABSs) [13,14] or disorder-induced bound states [15,16]. As for the chiral Majorana edge modes in quantum anomalous Hall (QAH)-superconductor junctions, the experimental observation of a half-integer quantized conductance plateau [17] has also been shown both theoretically [18,19] and experimentally [20] to have alternative non-Majorana origins, such as a good electric contact between the QAH film and the superconductor film [18], or the percolation of quantum Hall edges induced by magnetic disorders [19]. In the aspect of another important signature of MZMs, the 4π-periodic Josephson effect [21–24], the present observation of the missing first Shapiro step is not yet sufficient to conclude the existence of Majorana modes [25–36] . Therefore, the search for new smoking-gun signatures of MZMs is still highly desirable. Besides, the previously predicted transport signatures of MZMs under a bias originate from the probability of scattering amplitudes, but the signatures related to the phases of scattering amplitudes are still lacking.

In this work, we propose a smoking-gun signature of MZMs, a quantized Majorana pump (QMP) in semiconductor-superconductor heterostructures. The pump is formed by a Rashba spin-orbit coupled nanowire in proximity to an *s*-wave superconductor and in a magnetic field, sandwiched between two ferromagnetic leads as shown in Fig. 1. We show that, when the orientation of the magnetic field is rotated by 2π, an elementary charge e is pumped between two leads. The origin is that the phase of Andreev reflection amplitude is linearly determined by the orientation of magnetic field. The number of the pumped charge is related to the nontrivial winding number of the Andreev reflection amplitude. In the topologically trivial phase without MZM, the pumped charge decreases and deviates from the quantized value explosively. This QMP is analogous to, but better than the QMC in that it provides a more effective way to distinguish MZMs from PSABSs. The suggested methods to distinguish between MZMs and PSABSs include the measurements of nonlocality of MZMs [37,38], nonlocal conductance correlations from two ends [13,39], the shot noise correlations [40], the interferometry effect [41], and the π shift in the phase-biased supercurrent [42]. In our proposed pump, the pumped charge also decreases and deviates from the quantized value quickly for PSABSs due to the coupling between two PSABSs. This QMP provides a smoking-gun signature of MZMs and can rule out the origin of PSABSs in the same single setup.

In addition, although there have been several works that studied quantum pumps based on the systems involving MZMs [43–48], the quantized charge pump is still rare [47,48]. Despite a few theoretical proposals for topological

*phjfliu@gzhu.edu.cn
†jwang@seu.edu.cn

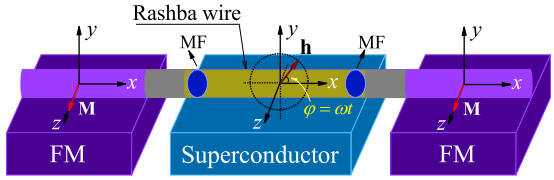

FIG. 1. Sketch of the quantized Majorana pump. A Majorana wire (a Rashba wire in proximity to an s-wave superconductor and in a magnetic field) is sandwiched between two ferromagnetic leads. The rotating magnetic field induces a rotating Zeeman field $\mathbf{h}$ in the x-y plane. The magnetization orientation of two ferromagnetic leads is along the z direction.

Thouless pump [47–53], the experimental evidence is only reported in cold atom systems [54,55], not yet observed in condensed matter systems. Our QMP provides also an ideal platform to realize topological single-electron pumps with the potential for realizing novel current standards in electrical metrology.

II. MODEL

The QMP is sketched in Fig. 1. The central Majorana wire is made by a Rashba wire in proximity to an s-wave superconductor and in a magnetic field. Two ferromagnetic leads are contacted to the Majorana wire at two sides. The magnetization orientation is along the z direction. The Majorana wire is in a rotating magnetic field which induces a rotating Zeeman field $\mathbf{h}$ in the x-y plane. The tight-binding Hamiltonian of the junction can be given by $H = H_{MW} + H_{L,R} + H_C$. Here the Hamiltonian of the Majorana wire is

$$\begin{aligned} H_{MW} = \sum_{i,\sigma,\sigma'} \Big\{ & (-\mu' + \boldsymbol{h}\cdot\boldsymbol{\sigma})_{\sigma\sigma'} c^\dagger_{i,\sigma} c_{i,\sigma'} \\ & - \left[\left(t_w + i\frac{\alpha}{a}\sigma_z \right)_{\sigma\sigma'} c^\dagger_{i,\sigma} c_{i+1,\sigma'} + \text{H.c.} \right] \Big\} \\ & + \sum_i [\Delta c^\dagger_{i,\uparrow} c^\dagger_{i,\downarrow} + \text{H.c.}], \end{aligned} \tag{1}$$

where $c^\dagger_{i,\sigma}$ ($c_{i,\sigma}$) creates (destroys) an electron at site i with spin σ, t_w is the hopping energy in the wire, $\mu' = \mu - 2t_w$ with μ being the chemical potential measured from the bottom of electronic band, $\boldsymbol{\sigma}$ are three Pauli matrices for spin and $\boldsymbol{h}$ is the rotating Zeeman field with $h_x = h\cos\omega t$ and $h_y = h\sin\omega t$, α is the Rashba coupling strength and a is the lattice constant, and Δ the superconducting pairing potential. The Hamiltonian of the left and right ferromagnetic leads is $H_{L,R} = \sum_{i,\sigma,\sigma'} \{(U_l - \mu' + m_z\sigma_z)_{\sigma\sigma'} c^\dagger_{i,\sigma} c_{i,\sigma'} - [t_l c^\dagger_{i,\sigma} c_{i+1,\sigma} + \text{H.c.}]\}$, where U_l is the electrostatic potential in two leads, m_z is the Zeeman splitting energy along the z axis, and t_l the hopping energy in leads. H_C describes the coupling between the wire and leads at two interfaces $H_C = -t_c \sum_{i,\sigma} c^\dagger_{i,\sigma} c_{i+1,\sigma} + \text{H.c.}$ with t_c the coupling strength.

In order to investigate the static conductance and dynamic pumped current, we need to calculate the instantaneous scattering matrix of the junction. Using the Fisher-Lee relation [56], the scattering matrix can be obtained based on the lattice Green's function technique by

$$S^{\alpha\beta}_{qp} = -\delta_{pq}\delta_{\alpha\beta} + i\left[\Gamma^\alpha_q\right]^{1/2} G^{\alpha\beta}_{qp} \left[\Gamma^\beta_p\right]^{1/2}. \tag{2}$$

Here, $\alpha, \beta \in \{e, h\}$ label the electron or hole and $p, q \in \{L, R\}$ represent the left and right leads. The matrix $S^{\alpha\beta}_{qp}$ denotes the scattering amplitude of the process where an incident particle β from lead p is scattered as a particle α in lead q. $\Gamma^{\alpha(\beta)}_{p(q)}$ is a block of the linewidth function $\Gamma_{p(q)} = i[\Sigma^r_{p(q)} - \Sigma^a_{p(q)}]$ with retarded/advanced self-energy $\Sigma^{r/a}_{p(q)}$ due to the coupling to the lead $p(q)$ which can be calculated numerically by the recursive method. $G^{\alpha\beta}_{qp}$ is the matrix block of the retarded Green's function of the Majorana wire which is determined by $G^r = [E - H_{MW} - \Sigma^r_L - \Sigma^r_R]^{-1}$. The local Andreev reflection (LAR) coefficient R_{he} can be calculated by

$$R_{he} = Tr\left\{\left[S^{h,e}_{L,L}\right]^\dagger S^{h,e}_{L,L}\right\} = Tr\left\{\Gamma^h_L G^{h,e}_{L,L} \Gamma^e_L \left[G^{h,e}_{L,L}\right]^\dagger\right\}. \tag{3}$$

The other scattering coefficients, T_{he}, T_{ee}, and R_{ee}, can also be obtained similarly. At zero temperature, when the Zeeman field $\boldsymbol{h}$ is fixed, the static differential conductance can be calculated by $G(E) = \frac{e^2}{h}(N - R_{ee} + R_{he})$ where N is the number of electron channels in leads and E is the energy of incident electrons and also the voltage bias. When the Zeeman field $\boldsymbol{h}$ is rotated adiabatically in the x-y plane with a frequency ω, the pumped current in a period $T_{\boldsymbol{h}} = 2\pi/\omega$ is [57]

$$\begin{aligned} i(E) = \frac{e}{2\pi T_{\boldsymbol{h}}} \int_0^{T_{\boldsymbol{h}}} \text{Im Tr} \Big[& \frac{dr_{ee}}{dt} r^\dagger_{ee} + \frac{dt_{ee}}{dt} t^\dagger_{ee} \\ & - \frac{dr_{he}}{dt} r^\dagger_{he} - \frac{dt_{he}}{dt} t^\dagger_{he} \Big] dt, \end{aligned} \tag{4}$$

where $r_{ee}, r_{he}, t_{ee}, t_{he}$ are the electronic scattering amplitudes corresponding to normal reflection, LAR, transmission, and cross Andreev reflection (CAR) processes, respectively. These four 2×2 matrices are obtained by Eq. (2). At finite temperature, the pumped current is counted by

$$I = -\int_{-\infty}^{\infty} \partial_E f(E) i(E) dE, \tag{5}$$

where $f(E) = [1 + \exp(\frac{E}{k_B T})]^{-1}$ is the Fermi distribution function.

III. QUANTIZED MAJORANA PUMP

At first, we consider a long Majorana wire sandwiched by two ferromagnetic leads with magnetization along the z direction, as shown in Fig. 1. When the Zeeman field in Majorana wire $\boldsymbol{h}$ is fixed in the x-y plane, the static differential conductance at zero temperature is shown in Fig. 2(a) as the function of the energy of electrons. The zero-bias conductance peak (ZBCP) is clearly exhibited and reaches the quantized value. The decrease in t_c only shrinks the width of ZBCP. When $\boldsymbol{h}$ is adiabatically rotated anticlockwise at zero bias, the pumped current is shown in Fig. 2(b) as the function of electronic energy. The current exhibits a similar zero-energy peak to ZBCP and reaches the quantized value e/T_h which messages that an elementary charge e is pumped in a cycle.

We can understand the quantized pump signal at zero energy as follows. In the long junction limit, the probabilities of transmission and CAR vanish. And due to the Zeeman

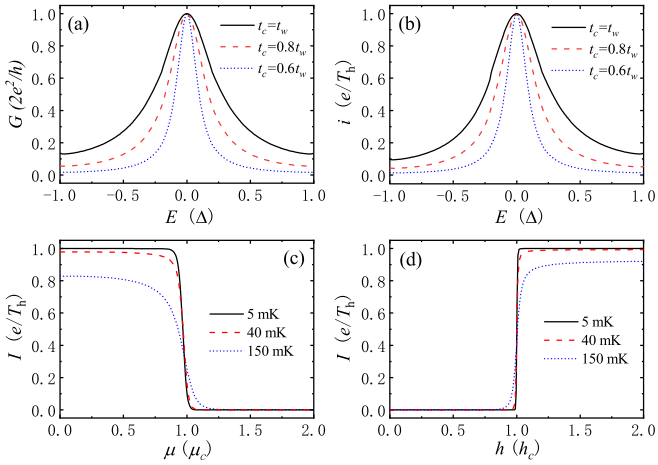

FIG. 2. (a) and (b) are the static differential conductance and the pumped current as functions of the energy of electrons at zero temperature, respectively. Various t_c are considered. (c) and (d) are the pumped current at various temperatures, as functions of the chemical potential (c) and the Zeeman field strength (d). The length of Majorana wire is $L = 2\mu m$ and the other parameters are $\Delta = 0.25$ meV, $t_w = t_l = 9.5$ meV, $\alpha = 40$ meV $\cdot$ nm, $a = 0.648nm$, $m_z = 2$ meV, $U_l = -0.95$ meV. In (a) and (b), $h = 2\Delta$, $\mu = 0.5\mu_c$ with $\mu_c = \sqrt{h^2 - \Delta^2}$. In (c), $t_c = t_w$, $h = 2\Delta$. In (d), $t_c = t_w$, $\mu = 4\Delta$ and $h_c = \sqrt{\mu^2 + \Delta^2}$.

splitting energy m_z, only the spin-down electronic band is occupied in two leads. In the presence of MZMs at zero energy, the incident spin-down electron is completely reflected to a spin-down hole, which is also the origin of QMC [58,59]. Therefore, only the Andreev reflection amplitude $r_{h\downarrow e\downarrow}$ contributes to the pumped current. Both our analytic derivation and numerical results show that $r_{h\downarrow e\downarrow}$ keeps its modulus to 1 but only decreases the argument by 2π during a pump period, as shown in the Supplemental Material [60]. Equation (2) makes it clear that the pumped charge number should be quantized to 1. The linear decreasing of the argument of $r_{h\downarrow e\downarrow}$ in time results in an important feature of this novel QMP that the time-resolved pumped current is constant in a period [60].

At finite temperature, the pumped current should be averaged over energy with the weight of the derivative of the Fermi function. At low enough temperature, the averaged current is still well quantized to 1, as shown in Figs. 2(c) and 2(d). Though, when the Rashba wire is in a topologically trivial phase without MZMs which does not satisfy the condition $h^2 > \mu^2 + \Delta^2$ [59], the pumped current decreases explosively to zero. Figures 2(c) and 2(d) show the pumping signal of this topological transition induced by μ and h, respectively. The vanishing pumped current can be explained in the following way. Without MZMs, the equal-spin Andreev reflection along the z axis is prohibited. Instead, the spin-down electron is normally reflected to a spin-down backwards electron. This normal reflection amplitude $r_{e\downarrow e\downarrow}$ keeps both modulus and argument unchanged during the rotation of $\boldsymbol{h}$, which has been numerically confirmed [60].

Note that the QMP has a topological origin. The topology is depicted by the winding number of the Andreev reflection matrix as [61]

$$w = \frac{1}{2\pi i}\oint d\{\ln[Det(r_{he})]\}, \tag{6}$$

where r_{he} is the 2×2 Andreev reflection amplitude matrix and $Det(r_{he})$ represents the determinant of r_{he}. The number of the pumped charge in a cycle is directly opposite to this winding number for a long junction. Although the single-electron pump [62–65] and even quantized pump [64,65] have been demonstrated experimentally, the topological Thouless charge pump have only been realized in cold-atom systems in optical superlattices [54,55], and simulated in a single-spin in a rotating field [66]. The real Thouless pump has not been reported in experiments on condensed matter systems. Our QMP provides an experimentally accessible platform for topological single-electron pumps which has the potential for realizing novel current standards in electrical metrology.

IV. DISTINCTION BETWEEN MZM AND PSABS

Next, we discuss the distinction between MZMs and topologically trivial PSABSs. To host PSABSs in the junction, we follow Refs. [13,14] to introduce a quantum dot (QD) potential at the left end of the Majorana wire $V = V_{\text{barrier}} + V_{\text{dot}}$. Here, $V_{\text{barrier}} = V_b[\Theta(x) - \Theta(x - L_b)]$ arises from the tunnel coupling between the left lead and the Majorana wire, and the QD spatial potential reads

$$V_{\text{dot}} = \frac{V}{2}\left[1 - \tanh\left(\frac{x - L_d}{\sigma_v}\right)\right], \tag{7}$$

where V is the height of the gate potential, L_d is the length of the quantum dot, and σ_v is the length scale over which V_{dot} varies. The induced superconducting pair potential is modified as

$$\Delta(x) = \frac{\Delta}{2}\left[1 - 2\Theta(x - L) + \tanh\left(\frac{x - L_d + \delta_x}{\sigma_\Delta}\right)\right], \tag{8}$$

in which δ_x denotes the extension of the pairing potential in the QD region, and σ_Δ is the length scale over which Δ varies. It is shown that this wire hosts MZMs for $h > h_c$ or PSABSs for $h < h_c$ with $h_c = \sqrt{\mu^2 + \Delta^2}$ [13,14].

In the case of $h < h_c$, two topologically trivial PSABSs locate at two ends of the quantum dot. Due to the narrow size of the dot, the coupling between two PSABSs is heavy, which induces the splitting of the conductance peak at zero energy. Figures 3(a) and 3(b) show the static differential conductance and the pumped current as functions of the energy of electrons at zero temperature. Two values of h are considered. For $h = 1.25h_c$, the zero energy peaks in both the conductance and the pumped current remains intact due to the presence of MZMs. For $h = 0.75h_c$, the wire becomes topologically trivial. However, because of the presence of PSABSs, the zero energy peaks still survive, only with a sharp dip at just zero energy. This dip arises from the finite coupling between two PSABSs due to their relatively short distance. While for the topological phase with $h > h_c$, the dip vanishes due to the nearly vanishing coupling between two MZMs located at two ends of the Majorana wire. It is noticeable that this sharp dip is difficult to measure due to the request for fine tuning of the bias in the conductance measurement. While for the QMP,

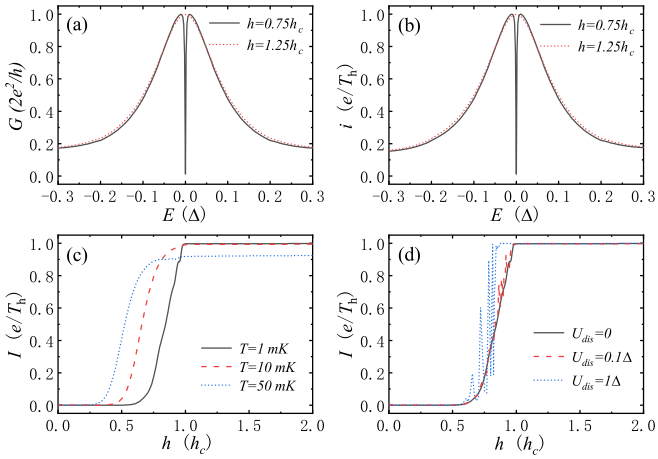

FIG. 3. (a) and (b) are the static differential conductances and the pumped currents as functions of the energy of electrons at zero temperature for the junction with a quantum dot, respectively. Two values of h are considered. (c) and (d) are the pumped currents as functions of the Zeeman field strength for various temperatures(c) or various disorder strengths (d), respectively. $V = 5.5\Delta$, $V_b = 16\Delta$, $L_b = 10$ nm, $L_d = 250$ nm, $L = 1\mu m$, and $\sigma_v = \sigma_\Delta = 12.5$ nm. The other parameters are the same as those in Fig. 2(d). In (d), the temperature is $T = 1$ mK.

the pump works in the zero-bias status because the current is driven by the rotating magnetic field instead of the bias. Therefore, the pump signal can focus on the dip at exact zero energy.

Figure 3(c) shows the pumped current as functions of the Zeeman field at various temperatures. At $T = 1$ mK, the pumped current keeps well quantized value for $h > h_c$. When h decreases and passes through the critical value h_c, the pumped current undergoes a sharp decreasing and finally goes to zero after a transition region. At higher temperatures, the transition regions are larger and the decreasing of the pumped current becomes more smooth. It is clearly shown that the sharp decreasing in the pumped current can distinguish MZMs from topologically trivial PSABSs.

Moreover, the robustness against disorders is also different for PSABSs and MZMs. Figure 3(d) illustrates the pumped currents as functions of the Zeeman field strength for various disorder strengths. The nonmagnetic Anderson random disorders are considered in the central Majorana wire. The nonmagnetic impurities are modeled by the random on-site potential $H_{\rm dis} = \sum_{i,\sigma} U_i c^\dagger_{i,\sigma} c_{i,\sigma}$, where U_i is the random potential uniformly distributed in the interval $[-U_{\rm dis}/2, U_{\rm dis}/2]$. It is shown that the quantized plateau for $h > h_c$ at low temperature $T = 1$ mK is robust against nonmagnetic disorders due to the topological nature of MZMs. By contrast, the pumped current fluctuates violently in the transition region, and depends on the particular disorder configuration in a sample. Finally, we argue that the extremely low temperature required to observe the sharp decrease in the pumped current around h_c can be improved one order higher by choosing a bigger superconducting gap and should be experimentally accessible.

V. EXPERIMENTAL FEASIBILITY

Finally, we comment on the experimental feasibility of our proposed QMP. The Majorana wire and the rotating magnetic field have been well established in experiments. The ferromagnetic leads can be realized by depositing Fe/Au [67] or EuS [68] on the semiconductor nanowire. This QMP should be operated in the adiabatic regime, i.e., $\hbar\omega \ll \Delta$. In this case, the transition between electronlike and holelike subbands due to the rotating magnetic field is ignorable. It is also noticeable that the Majorana wire considered in our QMP is narrow enough to exclude the multi-sub-band effect. For a wider wire with more than one subbands occupied, the orbital effects of the magnetic field should be considered [69,70]. We also investigated the influence of quantum dot parameters on the pumped current. It is shown that the quantum dot parameters, such as V and L_d, only affect the smoothness of the transition of the pumped current from 1 to 0 at the topologically critical point h_c [60]. And the Majorana wire length has an ignorable effect on the pumped current when the Majorana wire is long enough and hence the coupling between two MZMs vanishes. Besides, the QMP is insensitive to the electrostatic potential U_l in two leads, and will be observed if only there remains one spin subband (along the z direction) occupied in the leads.

We notice that the QMC is shown to be also possible due to disorder-induced bound states in two recent theoretical works [15,16]. But due to the topologically trivial nature, the coupling between these bound states are often much stronger than that between topological MZMs [37,38,71–73]. Therefore, the QMC owing to topologically trivial bound states will be split due to the partially separated nature of bound states. As a consequence, the QMP will decrease rapidly to zero. In this sense, we argue that our proposed QMP is a smoking gun signature of topological MZMs.

VI. CONCLUSIONS

In conclusion, we propose a QMP in Majorana wires sandwiched by two ferromagnetic leads. When the orientation of the Zeeman field in the Majorana wire is rotated by 2π, an elementary charge e is pumped between two leads. The quantized pump effect is attributed to the winding number of the spin-equal resonance Andreev reflection amplitude which keeps the modulus to 1 but changes the argument by 2π in a cycle. More importantly, the pump can also distinguish MZMs from PSABSs. In this sense, the QMP provides a smoking-gun signature of MZMs, as well as an ideal platform to realize topological single-parameter and single-electron charge pumps. This phase-related QMP effect will intrigue the field to pay attention to the phases of scattering amplitudes, and more phase-related transport phenomena, such as the anomalous Josephson effect.

ACKNOWLEDGMENTS

The work described in this paper is supported by the National Natural Science Foundation of China (NSFC, Grants No. 11774144, No. 11774006, and No. 11874221), and NBRP of China (No. 2012CB921300).

[1] A. Yu. Kitaev, Usp. Fiz. Nauk **44**, 131 (2001).
[2] J. Alicea, Rep. Prog. Phys. **75**, 076501 (2012).
[3] M. Leijnse and K. Flensberg, Semicond. Sci. Technol. **27**, 124003 (2012).
[4] C. W. J. Beenakker, Annu. Rev. Condens. Matter Phys. **4**, 113 (2013).
[5] S. D. Sarma, M. Freedman, and C. Nayak, npj Quantum Inf. **1**, 15001 (2015).
[6] R. Aguado, Riv. Nuovo Cimento Soc. Ital. Fis. **40**, 523 (2017).
[7] D. Litinski, M. S. Kesselring, J. Eisert, and F. von Oppen, Phys. Rev. X **7**, 031048 (2017).
[8] R. M. Lutchyn, E. P. A. M. Bakkers, L. P. Kouwenhoven, P. Krogstrup, C. M. Marcus, and Y. Oreg, Nat. Rev. Mater. **3**, 52 (2018).
[9] C. Schrade and L. Fu, Phys. Rev. Lett. **120**, 267002 (2018).
[10] H. Zhang, D. E. Liu, M. Wimmer, and L. P. Kouwenhoven, Nat. Commun. **10**, 5128 (2019).
[11] H. Zhang, C.-X. Liu, Sasa Gazibegovic, Di Xu, John A. Logan, Guanzhong Wang, Nick van Loo, Jouri D. S. Bommer, Michiel W. A. de Moor, Diana Car *et al.*, Nature (London) **591**, E30 (2021).
[12] H. Zhang, C.-X. Liu, S. Gazibegovic, D. Xu, J. A. Logan, G. Wang, N. van Loo, J. D. S. Bommer, M. W. A. de Moor, D. Car *et al.*, arXiv:2101.11456.
[13] C. Moore, T. D. Stanescu, and S. Tewari, Phys. Rev. B **97**, 165302 (2018).
[14] C. Moore, C. Zeng, T. D. Stanescu, and S. Tewari, Phys. Rev. B **98**, 155314 (2018).
[15] H. Pan, C.-X. Liu, M. Wimmer, and S. Das Sarma, arXiv:2102.02218v1.
[16] H. Pan and S. Das Sarma, arXiv:2102.07296v1.
[17] Q. L. He, L. Pan, A. L. Stern, E. C. Burks, X. Che, G. Yin, J. Wang, B. Lian, Q. Zhou, E. S. Choi *et al.*, Science **357**, 294 (2017).
[18] W. J. Ji and X. G. Wen, Phys. Rev. Lett. **120**, 107002 (2018).
[19] Y. Huang, F. Setiawan, and J. D. Sau, Phys. Rev. B **97**, 100501(R) (2018).
[20] M. Kayyalha, D. Xiao, R. Zhang, J. Shin, J. Jiang, F. Wang, Y.-F. Zhao, R. Xiao, L. Zhang, K. M. Fijalkowski *et al.*, Science **367**, 64 (2020).
[21] L. Fu and C. L. Kane, Phys. Rev. Lett. **100**, 096407 (2008).
[22] L. Fu and C. L. Kane, Phys. Rev. B **79**, 161408(R) (2009).
[23] H.-J. Kwon, K. Sengupta, and V. M. Yakovenko, Eur. Phys. J. B **37**, 349 (2003).
[24] L. Jiang, D. Pekker, J. Alicea, G. Refael, Y. Oreg, and F. von Oppen, Phys. Rev. Lett. **107**, 236401 (2011).
[25] J. Wiedenmann, E. Bocquillon, R. S. Deacon, S. Hartinger, O. Herrmann, T. M. Klapwijk, L. Maier, C. Ames, C. Brüne, C. Gould *et al.*, Nat. Commun. **7**, 10303 (2016).
[26] E. Bocquillon, R. S. Deacon, J. Wiedenmann, P. Leubner, T. M. Klapwijk, C. Brüne, K. Ishibashi, H. Buhmann, and L. W. Molenkamp, Nat. Nanotechnol. **12**, 137 (2017).
[27] R. S. Deacon, J. Wiedenmann, E. Bocquillon, F. Domínguez, T. M. Klapwijk, P. Leubner, C. Brüne, E. M. Hankiewicz, S. Tarucha, K. Ishibashi, H. Buhmann, and L. W. Molenkamp, Phys. Rev. X **7**, 021011 (2017).
[28] C. Li, J. C. de Boer, B. de Ronde, S. V. Ramankutty, E. van Heumen, Y. Huang, A. de Visser, A. A. Golubov, M. S. Golden, and A. Brinkman, Nat. Mater. **17**, 875 (2018).
[29] W. Yu, W. Pan, D. L. Medlin, M. A. Rodriguez, S. R. Lee, Zhi-qiang Bao, and F. Zhang, Phys. Rev. Lett. **120**, 177704 (2018).
[30] A.-Q. Wang, C.-Z. Li, C. Li, Z.-M. Liao, A. Brinkman, and D.-P. Yu, Phys. Rev. Lett. **121**, 237701 (2018).
[31] K. Le Calvez, L. Veyrat, F. Gay, P. Plaindoux, C. B. Winkelmann, H. Courtois, and B. Sacépé, Commun. Phys. **2**, 4 (2019).
[32] P. Schüffelgen, D. Rosenbach, C. Li, T. W. Schmitt, M. Schleenvoigt, A. R. Jalil, S. Schmitt, J. Kölzer, M. Wang, B. Bennemann *et al.*, Nat. Nanotechnol. **14**, 825 (2019).
[33] D. Laroche, D. Bouman, D. J. van Woerkom, A. Proutski, C. Murthy, D. I. Pikulin, C. Nayak, R. J. J. vanGulik, J. Nygård, P. Krogstrup, L. P. Kouwenhoven, and A. Geresdi, Nat. Commun. **10**, 245 (2019).
[34] R. Yano, M. Koyanagi, H. Kashiwaya, K. Tsumura, H. T. Hirose, T. Sasagawa, Y. Asano, and S. Kashiwaya, J. Phys. Soc. Jpn. **89**, 034702 (2020).
[35] Y. Takeshige, S. Matsuo, R. S. Deacon, K. Ueda, Y. Sato, Y.-F. Zhao, L. Zhou, C.-Z. Chang, K. Ishibashi, and S. Tarucha, Phys. Rev. B **101**, 115410 (2020).
[36] C. Knapp, A. Chew, and J. Alicea, Phys. Rev. Lett. **125**, 207002 (2020).
[37] E. Prada, R. Aguado, and P. San-Jose, Phys. Rev. B **96**, 085418 (2017).
[38] M.-T. Deng, S. Vaitiekėnas, E. Prada, P. San-Jose, J. Nygård, P. Krogstrup, R. Aguado, and C. M. Marcus, Phys. Rev. B **98**, 085125 (2018).
[39] Y.-H. Lai, J. D. Sau, and S. Das Sarma, Phys. Rev. B **100**, 045302 (2019).
[40] J. Manousakis, C. Wille, A. Altland, R. Egger, K. Flensberg, and F. Hassler, Phys. Rev. Lett. **124**, 096801 (2020).
[41] M. Hell, K. Flensberg, and M. Leijnse, Phys. Rev. B **97**, 161401(R) (2018).
[42] O. A. Awoga, J. Cayao, and A. M. Black-Schaffer, Phys. Rev. Lett. **123**, 117001 (2019).
[43] A. Keselman, L. Fu, A. Stern, and E. Berg, Phys. Rev. Lett. **111**, 116402 (2013).
[44] M. Alos-Palop, R. P. Tiwari, and M. Blaauboer, Phys. Rev. B **89**, 045307 (2014).
[45] Ganesh C. Paul and A. Saha, Phys. Rev. B **95**, 045420 (2017).
[46] K. M. Tripathi, S. Rao, and S. Das, Phys. Rev. B **99**, 085435 (2019).
[47] M. Gibertini, R. Fazio, M. Polini, and F. Taddei, Phys. Rev. B **88**, 140508(R) (2013).
[48] Q.-F. Liang, Z. Wang, and X. Hu, Phys. Rev. B **89**, 224514 (2014).
[49] D. J. Thouless, Phys. Rev. B **27**, 6083 (1983).
[50] J. Wang and J.-F. Liu, Phys. Rev. B **95**, 205433 (2017).
[51] J. Wang, J. F. Liu, and C. S. Ting, Phys. Rev. B **100**, 075402 (2019).
[52] Paolo A. Erdman, Fabio Taddei, Joonas T. Peltonen, Rosario Fazio, and Jukka P. Pekola, Phys. Rev. B **100**, 235428 (2019).
[53] M.-J. Wang, J. Wang, and J.-F. Liu, New J. Phys. **22**, 013042 (2020).
[54] M. Lohse, C. Schweizer, O. Zilberberg, M. Aidelsburger, and I. Bloch, Nat. Phys. **12**, 350 (2016).
[55] S. Nakajima, T. Tomita, S. Taie, T. Ichinose, H. Ozawa, L. Wang, M. Troyer, and Y. Takahashi, Nat. Phys. **12**, 296 (2016).
[56] D. S. Fisher and P. A. Lee, Phys. Rev. B **23**, 6851 (1981).

[57] M. Büttiker, A. Prêre, and H. Thomas, Z. Phys. B: Condens. Matter **94**, 133 (1994).
[58] K. T. Law, P. A. Lee, and T. K. Ng, Phys. Rev. Lett. **103**, 237001 (2009).
[59] J. J. He, T. K. Ng, P. A. Lee, and K. T. Law, Phys. Rev. Lett. **112**, 037001 (2014).
[60] See Supplemental Material at http://link.aps.org/supplemental/10.1103/PhysRevB.103.195407 for the scattering amplitudes of the pump junction, the time-resolved pumped current in a period, and the influence of quantum dot parameters on the pumped current.
[61] J. E. Avron, A. Elgart, G. M. Graf, and L. Sadun, J. Stat. Phys. **116**, 425 (2004).
[62] M. Switkes, C. M. Marcus, K. Campman, and A. C. Gossard, Science **283**, 1905 (1999).
[63] J. M. Shilton, V. I. Talyanskii, M. Pepper, D. A. Ritchie, J. E. F. Frost, C. J. B. Ford, C. G. Smith, and G. A. C. Jones, J. Phys. Condens. Matter **8**, L531 (1996).
[64] M. D. Blumenthal, B. Kaestner, L. Li, S. Giblin, T. J. B. M. Janssen, M. Pepper, D. Anderson, G. Jones, and D. A. Ritchie, Nat. Phys. **3**, 343 (2007).
[65] B. Kaestner, V. Kashcheyevs, S. Amakawa, M. D. Blumenthal, L. Li, T. J. B. M. Janssen, G. Hein, K. Pierz, T. Weimann, U. Siegner, and H. W. Schumacher, Phys. Rev. B **77**, 153301 (2008).
[66] W. Ma, L. Zhou, Q. Zhang, M. Li, C. Cheng, J. Geng, X. Rong, F. Shi, J. Gong, and J. Du, Phys. Rev. Lett. **120**, 120501 (2018).
[67] Z. Yang, B. Heischmidt, S. Gazibegovic, G. Badawy, D. Car, P. A. Crowell, E. P. A. M. Bakkers, and V. S. Pribiag, Nano Lett. **20**, 3232 (2020).
[68] S. Vaitiekėnas, Y. Liu, P. Krogstrup, and C. M. Marcus, Nat. Phys. **17**, 43 (2021).
[69] M. P. Nowak and P. Wójcik, Phys. Rev. B **97**, 045419 (2018).
[70] P. Wójcik and M. P. Nowak, Phys. Rev. B **97**, 235445 (2018).
[71] L. S. Ricco, M. de Souza, M. S. Figueira, I. A. Shelykh, and A. C. Seridonio, Phys. Rev. B **99**, 155159 (2019).
[72] E. Prada, P. San-Jose, M. W. A. de Moor, A. Geresdi, E. J. H. Lee, J. Klinovaja, D. Loss, Jesper Nygård, R. Aguado, and L. P. Kouwenhoven, Nat. Rev. Phys. **2**, 575 (2020).
[73] A. Vuik, B. Nijholt, A. R. Akhmerov, and M. Wimmer, Sci. Post Phys. **7**, 061 (2019).